Available online at www.sciencedirect.com
SCIENCE DIRECT
Journal of Photochemistry and Photobiology A: Chemistry 174 (2005) 207–213
Journal of Photochemistry and Photobiology A:Chemistry
www.elsevier.com/locate/jphotochem

Raman spectroscopic studies on interactions of water soluble cationic oxovanadyl (IV) *meso*-tetrakis(1-methylpyridium-4-yl) porphyrin with nucleic acids

Dae Won Cho [a,*], Dae Hong Jeong [b], Jae-Hong Ko [c], Seog K. Kim [c], Minjoong Yoon [d,**]

[a] *Department of Chemistry, Seonam University, Namwon, Jeonbuk 590-711, Korea*
[b] *Department of Chemistry Education and Nano-Systems Institute (NSI-NCRC), Seoul National University, Seoul 151-742, Korea*
[c] *Department of Chemistry, Yeungnam University,Kyoungsan, Kyoungbuk 712-749, Korea*
[d] *Department of Chemistry, Chungnam National University, Daejeon 305-764, Korea*

Received 16 October 2004; received in revised form 24 February 2005; accepted 28 February 2005
Available online 11 April 2005

Abstract

Interactions of water soluble cationic oxovanadyl (IV) *meso*-tetrakis(1-methylpyridium-4-yl)porphyrin ($OV^{IV}(TMPyP)^{4+}$) with double stranded poly[d(A-T)$_2$], poly[d(G-C)$_2$] nucleotides and calf thymus DNA were studied by the Raman spectroscopic techniques as well as the polarization spectroscopic measurements. The ground state Raman bands of $OV^{IV}(TMPyP)^{4+}$ observed in the presence of poly[d(A-T)$_2$] were almost the same as those observed in a pure water solution except the slightly up-shifted Raman band (963 cm^{-1}) which is ascribed to the V─O stretching mode of six-coordinated complex, $OV^{IV}(H_2O)(TMPyP)^{4+}$. On the other hand, in the presence of poly[d(G-C)$_2$], a markedly up-shifted Raman band was observed at 992 cm^{-1}, indicating that $OV^{IV}(TMPyP)^{4+}$ interacts with poly[d(G-C)$_2$] by losing the sixth axial ligand. In the presence of calf thymus DNA, the V─O stretching band was observed to be resulted by combination of those observed in poly[d(A-T)$_2$] and poly[d(G-C)$_2$]. The polarization spectroscopic studies with these results imply that $OV^{IV}(TMPyP)^{4+}$ interacts with DNA in different groove binding patterns originated from the formation of five-coordinated adducts in the G-C pair-rich regions and six-coordinated adducts in the A-T pair-rich regions. The down-shifts of core-size sensitive transient Raman bands (ν_2 and ν_4 modes) in the presence of nucleic acids illustrate an increase of the core-size of porphyrin macrocycle in the excited triplet state. The transient Raman bands related to pyridine group were observed, and they are interpreted to be due to the excited-state charge transfer from porphyrin ring to peripheral substituents.

Keywords: Raman spectroscopy; DNA; Oxovanadyl (IV) *meso*-tetrakis(1-methylpyridium-4-yl)porphyrin

1. Introduction

Interaction of porphyrins derivatives with DNA has been an interesting subject since the pioneer work of Fiel [1] and Pasternack and Gibbs [2]. Porphyrins have served as excellent probe molecules to monitor the structure and dynamics of nucleic acids as well as proteins. Particularly, water-soluble metalloporphyrins have drawn much attention in the field of photodynamic therapy. It is also known that a direct interaction and strong binding of metallo *meso*-tetrakis(1-methylpyridium-4-yl)porphyrin ($(M\text{-}TMPyP)^{4+}$) with DNA is involved in the biochemical mechanism for its selective uptake [3,4]. Furthermore, interactions of some water-soluble metalloporphyrins such as Au(III), Pt(II), Pd(II), and other heavy metal derivatives of $H_2(TMPyP)^{4+}$ with nucleic acids have also been extensively investigated by using NMR, steady-state and time-resolved fluorescence, and resonance Raman techniques, even though a number of questions for the excited-state interactions of the metalloporphyrins as well as in the ground-state remain to be addressed. Particularly, the interaction of oxometallo-porphyrins with

* Corresponding author. Tel.: +82 636200175; fax: +82 636200113.
** Co-corresponding author.
E-mail addresses: dwcho@seonam.ac.kr (D.W. Cho), mjyoon@cnu.ac.kr (M. Yoon).

1010-6030/$ – see front matter © 2005 Elsevier B.V. All rights reserved.
doi:10.1016/j.jphotochem.2005.02.011

DNA has not been systematically studied as compared to the interactions with the active sites of heme protein such as peroxidases, catalases, and cytochrome P450's [5–8].

The oxovanadyl porphyrins contain a stable O–V bond, serve as convenient model systems for more active ferryl-oxo porphyrins [9] and are widely distributed as naturally occurring components in petroleum deposits and source rocks [10]. Such geoporphyrins are of biological origin, and their diagnosis provides a useful molecular fossils record of past environmental conditions in these geological formations. It is also known that their coordination chemistry plays an important role in catalytic deactivation in hydrotreating processes [11]. Oxovanadyl porphyrins also act as the photoactive components in electrophotography applications [12].

Oxovanadyl (IV) porphyrins are paramagnetic d^1 complexes and consequently can be expected to exhibit peculiar photophysical behaviors [13]. An unpaired electron in the d_{xy} orbital for oxovanadyl porphyrins results in a splitting of the porphyrin ring triplet state arising from a strong interaction between the π electronic system of the porphyrin ring and the unpaired electron in the metal d_{xy} orbital. The resultant ($^2T/^4T(\pi, \pi^*)$) states probably play significant roles in the relaxation dynamics of photoexcited oxovanadyl porphyrins, since the spin states of the lowest excited and ground porphyrin ring states are doublet ($^2S_1$ versus $^2S_0$) [14]. Furthermore, the unpaired electron can also invoke several charge transfer transitions such as ring-to-metal (π–d), metal-to-ring (d–π), metal-to-metal (d–d), and their mixtures [13]. However, the detailed electronic nature of the quenching state of oxovanadyl porphyrins is still controversial [15].

The resonance Raman (RR) studies of oxovanadyl porphyrins have been carried out in a great detail [16–20]. Particularly, Spiro and coworkers [20] exploited the H-bonding and the axial ligand interactions in the ground state of oxovanadyl porphyrins using the RR spectroscopy. The V–O Raman band of oxovanadyl porphyrins has been known to have a strong correlation with the axial ligation and also its electronic configuration. The frequency of the ν(V–O) mode depends on the nature of the electronic structure, and the solvent also plays important roles. The presence and nature of a (sixth) *trans*-axial ligand can have a substantial effect on the frequency of the ν(V–O) mode. However, the photophysical behaviors of photoexcited oxovanadyl porphyrins have not been fully understood in the previous studies performed by the RR spectroscopy [18]. Thus, there are necessities for further investigations with the transient RR spectroscopy, which can provide direct information on the strength of the oxo-metal bond and the electronic nature of porphyrin macrocycles in the excited state.

In this work, we have examined the transient RR and the ground-state RR spectral properties of tetracationic oxovanadyl(IV) *meso*-tetrakis(1-methylpyridium-4-yl) porphyrin ($OV^{IV}(TMPyP)^{4+}$) (see Scheme 1) in the presence of double stranded poly[d(A-T)$_2$], poly[d(G-C)$_2$] polynucleotides and calf thymus DNA solutions. The binding patterns of the metalloporphyrins with DNA in the excited state as well as in the ground state are discussed based on the relative Raman frequency changes of $OV^{IV}(TMPyP)^{4+}$ as the porphyrin interacts with different base pairs of DNA.

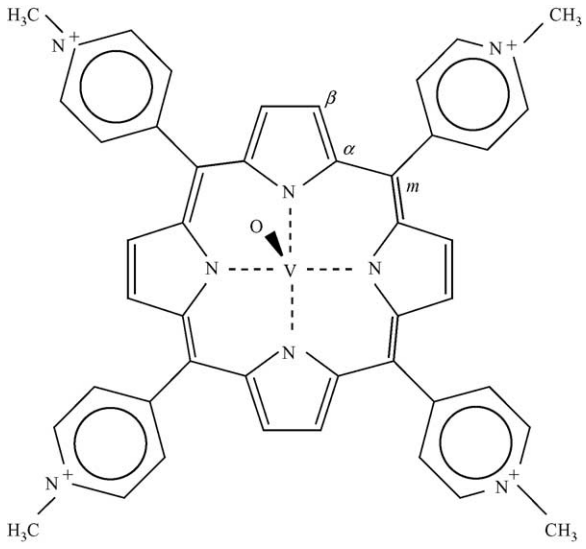

Scheme 1.

2. Experimental

2.1. Chemicals and preparation

$OV^{IV}(TMPyP)^{4+}$ was purchased from the Porphyrin Products (Logan, Utah). Distilled water was further purified using on a deionizer (ELGA, PL5241). Poly[d(A-T)$_2$], poly[d(G-C)$_2$] and calf thymus DNA were obtained from Sigma Aldrich Co. Each DNA was used without further purification. All experiments were carried out at room temperature in a phosphate buffer at pH 7 (ionic strength = 0.1 M). The DNA concentration was determined by measuring the absorbance at 260 nm. The base pairs/porphyrin ratio was ca. 40. The final porphyrin concentration was ca. 3 μM. The porphyrin stock solution was added to DNA solution and kept standing for 30 min before spectral measurements.

2.2. Transient Raman spectroscopy

The transient RR measurement set-up was previously described in detail [21,22]. The Raman spectra were measured by photoexcitation with 416 nm pulses generated by the hydrogen Raman shifting of the third harmonics (355 nm) from a nanosecond Q-switched Nd:YAG laser. The sample solution was flowed through a glass capillary tube at a rate sufficient enough to ensure that each laser pulse encounters a fresh volume of the sample. The Raman signals were collected with a single pass spectrograph (Acton Research 500i) equipped with a charge coupled device (PI LN/CCD 1152E).

One-color transient Raman spectra were obtained by the difference spectrum between intense (ca. 0.2 mJ/pulse) and weak (ca. 0.01 mJ/pulse) laser pulse excitations. The spectral features for the ground state porphyrins were subtracted to yield the excited state Raman spectra, using a subtraction factor sufficient enough to avoid any negative features.

2.3. Polarized spectroscopy

Although porphyrins do not possess any chiral center, CD spectrum can be induced by interaction between the porphyrin's electric transition moments and chirally arranged DNA base. CD spectra of the porphyrin-polynucleotide complexes were recorded on a Jasco 815 spectropolarimeter. The signal was averaged over an appropriate number of scans.

Linear dichroism (LD) is defined by difference in absorbance by an oriented sample between the parallel ($A_{||}$) and perpendicular ($A_{\perp}$) polarized light [23–25]. The measured LD is divided by isotropic absorption to give reduced LD (LD^r), which is related to the angle, α, that specifies the orientation of the transition moment of drug relative to the local DNA helix, as shown in the following equation:

$$LD^r = \frac{LD}{A} = \frac{A_{\parallel} - A_{\perp}}{A} = \frac{3}{2}S(3\cos^2\alpha - 1)$$

where S is the orientation factor such that $S = 1$ for perfect orientation and $S = 0$ for random orientation. It can be calculated by assuming the angle of 86° between the $\pi \rightarrow \pi^*$ transition of the DNA base and the DNA helix axis [26]. The LD spectra were recorded on a Jasco J 715 spectropolarimeter. For LD measurement, a flow-orienting Cuvette cell device with inner-rotating cylinder was used as described by Nordén and Seth [27]. The polarized light spectra were averaged over several scans when necessary.

3. Results and discussion

Fig. 1 shows the absorption spectra of $OV^{IV}(TMPyP)^{4+}$ in the presence of polynucleotides, exhibiting a Soret band located at 435 and 443 nm and visible Q-bands located in the range of 550–620 nm. The absorption bands of $OV^{IV}(TMPyP)^{4+}$ in the presence of various polynucleotides and DNA are summarized in Table 1. The Soret band (435 nm) of $OV^{IV}(TMPyP)^{4+}$ in poly[d(G-C)$_2$] solution is blue-shifted as compared to the one (443 nm) observed in

Table 1
UV-visible spectral data for the $OV^{IV}(TMPyP)^{4+}$ in pH 7 aqueous and DNA solutions

Complex	λ (nm)			
	pH 7	Poly[d(G-C)$_2$]	Poly[d(A-T)$_2$]	Calf thymus
$OV^{IV}(TMpy\text{-}P)^{4+}$	442	435	443	441
	564	557	566	564
	602	590	603	600

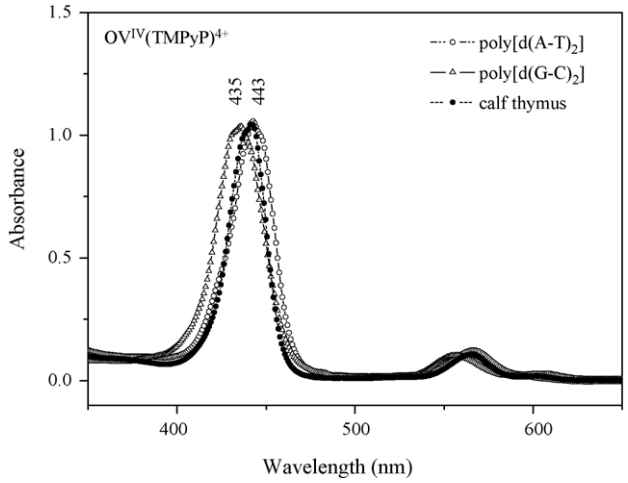

Fig. 1. Absorption spectra of $OV^{IV}(TMPyP)^{4+}$ in poly[d(A-T)$_2$], poly[d(G-C)$_2$] and calf thymus solution.

poly[d(A-T)$_2$] solution which is similar to that observed in pure water, reflecting that the interaction of the metallo-$(TMPyP)^{4+}$ with poly[d(G-C)$_2$] is different from that with poly[d(A-T)$_2$] in pH 7 aqueous solution. The absorption changes of Soret and Q bands in calf thymus solution intermediate between in poly[d(G-C)$_2$] and in poly[d(A-T)$_2$]. However, the absorption maxima are more similar to that in poly[d(A-T)$_2$] than that in poly[d(G-C)$_2$]. This result indicates that $OV^{IV}(TMPyP)^{4+}$ interact with d(A-T)$_2$ rich regions much more strongly than with d(G-C)$_2$ rich regions.

In order to explore the interaction patterns, the CD and LD spectra of the aqueous solution of $OV^{IV}(TMPyP)^{4+}$ measured in the presence of DNA, poly[d(A-T)$_2$] and poly[d(G-C)$_2$] were depicted in Figs. 2 and 3, respectively. When $OV^{IV}(TMPyP)^{4+}$ is associated with DNA and poly[d(A-T)$_2$], a positive CD signal in the Soret absorption

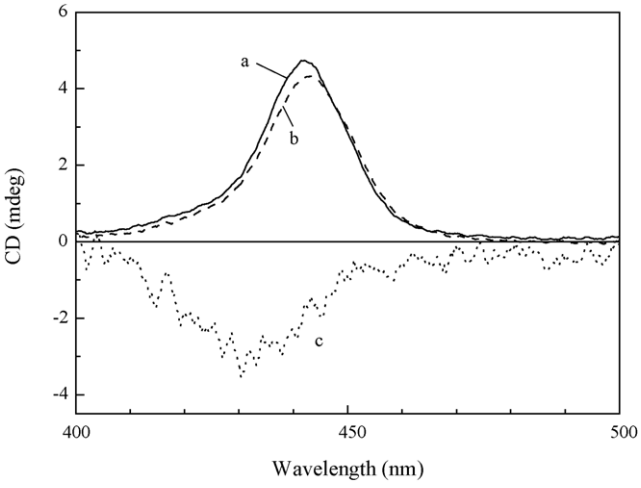

Fig. 2. CD spectrum of $OV^{IV}(TMPyP)^{4+}$ complexed with various polynucleotides in the Soret absorption band. (a) DNA, (b) poly[d(A-T)$_2$], (c) poly[d(G-C)$_2$]. That of the $OV^{IV}(TMPyP)^{4+}$-poly[d(G-C)$_2$] complex is ten times enlarged for easy of comparison. [polynucleotide] = 120 μM base pair and [porphyrin] = 3 μM.

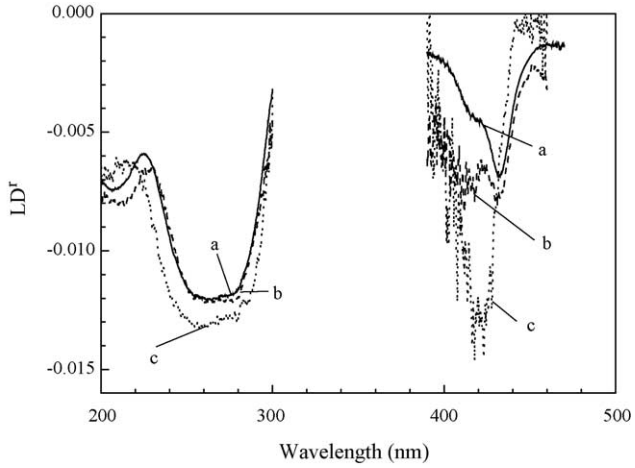

Fig. 3. LD^r spectrum of the $OV^{IV}(TMPyP)^{4+}$ complexed with various polynucleotides. (a) DNA, (b) poly[d(A-T)$_2$], (c) poly[d(G-C)$_2$]. That of the $OV^{IV}(TMPyP)^{4+}$-poly[d(A-T)$_2$] and -poly[d(G-C)$_2$] complex is enlarged by 6 and 15 times, respectively, for easy of comparison. [polynucleotide] = 120 μM base pair and [porphyrin] = 3 μM.

region was observed. CD spectral features for both complexes are similar, indicating that the interaction patterns of $OV^{IV}(TMPyP)^{4+}$ with DNA and poly[d(A-T)$_2$] are similar. A positive CD signal in the Soret region upon binding to DNA is usually attributed to the groove binding mode without any stacking. Similar CD spectra of $OV^{IV}(TMPyP)^{4+}$ have been reported [28]. Being consistent with that in [28], the LD spectra of the $OV^{IV}(TMPyP)^{4+}$-DNA and $OV^{IV}(TMPyP)^{4+}$-poly[d(A-T)$_2$ exhibit the strong wavelength-dependent LD^r in the Soret region, indicating that interactions of B_x and B_y transition of the porphyrin molecule with DNA are different. The degeneracy in the absorption band has been removed upon binding to DNA. The shape of the LD^r spectrum of the $OV^{IV}(TMPyP)^{4+}$-DNA and $OV^{IV}(TMPyP)^{4+}$-poly[d(A-T)$_2$] is similar. This means that the binding geometry of $OV^{IV}(TMPyP)^{4+}$ to DNA and poly[d(A-T)$_2$] is almost identical. Together with CD result, it is conceivable that $OV^{IV}(TMPyP)^{4+}$ bind at the groove of DNA and poly-[d(A-T)$_2$] and the binding geometry of porphyrin relative to both polynucleotide is almost identical. It has recently been known that groove binding of TMPyP occurs at the minor groove [29,30].

On the other hand, the $OV^{IV}(TMPyP)^{4+}$ in poly[d(G-C)$_2$] solution exhibited a weak negative CD signal in the same region. The negative CD signal seems to imply that the porphyrin could be intercalated into the base pair of poly-[d(G-C)$_2$]. If the porphyrin is really intercalated between the base pair, the reduced LD (LD^r) spectrum in the porphyrin absorption region should be wavelength-independent with its magnitude comparable or larger than that in the DNA absorption region. However, the $OV^{IV}(TMPyP)^{4+}$-poly[d(G-C)$_2$] complex also exhibited the wavelength-dependent LD^r spectrum in the Soret band with its magnitude smaller than that in the DNA absorption region. Therefore, despite the negative CD signal, $OV^{IV}(TMPyP)^{4+}$ is ascribed to be bound

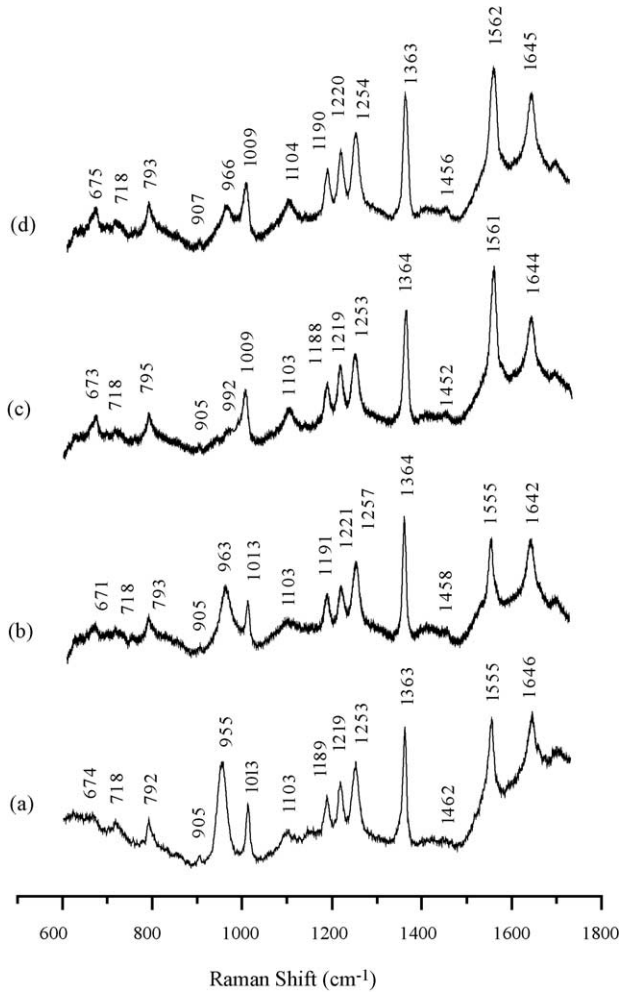

Fig. 4. Resonance Raman spectra of $OV^{IV}(TMPyP)^{4+}$ with the low-power (ca. 0.01 mJ/pulse) probe pulses at 416 nm: (a) in phosphate buffer solution (pH 7); (b) in poly[d(A-T)$_2$]; (c) in poly[d(G-C)$_2$]; and (d) in calf thymus.

at the groove site of poly[d(G-C)$_2$]. However, the angle between the porphyrin's molecular plane relative to the DNA helix in $OV^{IV}(TMPyP)^{4+}$-poly[d(G-C)$_2$] complex is considerably different from those in $OV^{IV}(TMPyP)^{4+}$-DNA and -poly[d(A-T)$_2$] complex.

Fig. 4a shows the ground state RR spectra of $OV^{IV}(TMPyP)^{4+}$ in pH 7 aqueous solution recorded by a very low-power nanosecond pulse excitation at 416 nm. The Raman bands are readily assigned with reference to the normal mode analysis of similar metallo-$(TMPyP)^{4+}$s [31–33]. The porphyrin macrocyclic bands are assigned as follows: the ν_2, ν_4, and $\nu(C_\alpha{-}C_m)$ modes are assigned to the bands at 1555, 1363, and 1013 cm^{-1}, respectively (see Table 2). The pyridine bands are also observed: $\delta(C_m{-}Pyr)$ at 1253 cm^{-1}, $\delta(Pyr)$ at 1219 cm^{-1}, $\delta(Pyr) + \nu(N^+{-}CH_3)$ at 1189 cm^{-1} and $\nu(C{-}C)_{Pyr} + \nu(N^+{-}CH_3)$ at 792 cm^{-1}, respectively. On the other hand, the strong 955 cm^{-1} band in pH 7 aqueous solution is assigned to the V–O stretching mode of the six-coordinate aqua adduct, $OV^{IV}(H_2O)(TMPyP)^{4+}$ [20]. The V–O bond is considered to be resulted from σ-donor

Table 2
Raman frequencies (cm^{-1}) and band assignments of $OV^{IV}(TMPyP)^{4+}$[a,b,c]

$OV^{IV}(TMPyP)^{4+}$				
Assignment	pH 7	Poly[d(G-C)$_2$]	Poly[d(A-T)$_2$]	Calf thymus
ϕ_4, δ(pyr)	1646 (−4)	1644 (−10)	1642 (0)	1645 (−6)
ν_2, $\nu(C_\beta C_\beta)$	1555 (−5)	1561 (−8)	1555 (−2)	1562 (−13)
ν_3, $\nu(C_\alpha C_\beta)$	1462	1452	1458	1456
ν_4, $\nu(C_\alpha N)$	1363 (−13)	1364 (−8)	1364 (−7)	1363 (−7)
ν_1, $\delta(C_m$-pyr)[a]	1253 (−4)	1253 (−8)	1257 (−2)	1254 (−3)
δ(pyr)[a]	1219 (0)	1219 (0)	1221 (+5)	1220 (−3)
δ(pyr) + $\nu(N^+{-}CH_3)$[a]	1189 (0)	1188 (−5)	1191 (0)	1190 (−5)
ν_9, $\delta(C_\beta{-}H)$	1103 (−7)	1103 (5)	1103 (0)	1104(−13)
ν_6, $\nu(C_\alpha{-}C_m)$	1013	1009	1013	1009
ν(OV)		992		∼992
ν(OV)···(H_2O)[d]	955			
ν(OV)···(H_2O)[e]			963	966
ν_7, $\delta(CC)_{ph}$	905 (−3)	905 (0)	905 (0)	907 (−4)
$\nu(CC)_{pyr}$ + $\nu(N^+{-}CH_3)$[a]	792 (0)	795 (−5)	793 (−2)	793

[a] From Ref. [31].
[b] From Ref. [32].
[c] From Ref. [33].
[d] From Ref. [20].
[e] In DNA values in parentheses are shifted values in the excited state.

interaction between the filled O^{2-} p_z orbital and the empty V^{4+} d_z^2 orbital, and π-donor interactions between the filled p_x and p_y orbitals and the empty d_{xz} and d_{yz} orbitals. This builds up a formal V–O triple bond, reflected in the high frequency stretching mode at ∼1000 cm^{-1}. The V–O bond strength is affected by axial ligation of the coordinating solvents. The V–O bond becomes weak by electron donation from the sixth ligand (L), which reduces the O → V donation: L and O compete for the same V acceptor orbital (*trans*-effect [34]).

In the poly[d(A-T)$_2$] solution (Fig. 4b), most of the Raman bands are similar to those in pure water solution with a slightly up-shift of the V–O stretching band appearing 963 cm^{-1}, as expected from the absorption spectra. This indicates that the 963 cm^{-1} band in poly[d(A-T)$_2$] is attributed to the V–O stretching mode of six-coordinate adduct, $OV^{IV}(H_2O)(TMPyP)^{4+}$. This observation implies that the microenvironment in poly[d(A-T)$_2$] is slightly nonpolar as compared with aqueous solution according to the outside groove binding. On the other hand, the V–O stretching band in poly[d(G-C)$_2$] solution (Fig. 4c) is markedly up-shifted to 992 cm^{-1} as compared with that observed in pure water. Previous studies for many other metallo-$(TMPyP)^{4+}$ suggest that the intercalation of tetracationic porphyrin inside the poly[d(G-C)$_2$] strand occurs. In general, free base porphyrin and square planar metalloporphyrins such as Ni^{2+}- and Cu^{2+}-porphyrins intercalate between the base pairs of DNA, while metalloporphyrins such as Mn^{3+}-, Fe^{3+}- and Co^{3+}-porphyrins having axial ligation site or those with bulky substituents on the periphery of the structure are prohibited to be intercalated. Therefore, in case of oxovanadyl porphryin having the axial ligation site O–V, intercalation is not probable in poly[d(G-C)$_2$]. Nevertheless, it is likely to form the five-coordinate complex, $OV^{IV}(TMPyP)^{4+}$ since the V–O stretching band in poly[d(G-C)$_2$] solution shows large up-shift by approximately 37 cm^{-1} from that in pure water. The large up-shifted V–O stretching band and the loss of Raman intensity in poly[d(G-C)$_2$] correspond to the loss of the sixth axial ligand through the interaction between the $OV^{IV}(TMPyP)^{4+}$ and poly[d(G-C)$_2$], forming a stronger VO bond. Similar phenomena of five-coordinate $OV^{IV}(TMPyP)^{4+}$ complex has been reported [35]. The ground state Raman spectrum of OV^{IV}TMPyP in calf thymus DNA solution is shown in Fig. 4d. Two characteristic Raman bands at 966 and 1009 cm^{-1} are observed. The former could be easily assigned to the V–O stretching mode of the six-coordinate adduct, $OV^{IV}(H_2O)(TMPyP)^{4+}$ in A-T pair rich region. The latter band is attributed to the $\nu(C_\alpha{-}C_m)$ stretch. On the other hand, The broadening of band (fwhm = 18 cm^{-1}) at 1009 cm^{-1} in calf thymus or poly[d(G-C)$_2$] solution can be observed, comparing with that (fwhm = 10 cm^{-1}) in pH 7 or poly[d(A-T)$_2$] solution. Therefore, in $OV^{IV}(TMPyP)^{4+}$ containing calf thymus or poly[d(G-C)$_2$], we suggest that the V–O stretching at ∼992 cm^{-1} of the five-coordinate adduct overlap with the $\nu(C_\alpha{-}C_m)$ stretching band.

Fig. 5a presents the transient Raman spectrum of $OV^{IV}(TMPyP)^{4+}$ in pH 7 aqueous solution obtained by the high-power 416 nm single pulse excitation. The Raman spectral features for the ground state $OV^{IV}(TMPyP)^{4+}$ were subtracted to yield the excited state Raman spectrum using a subtraction factor sufficient enough to avoid any negative feature. The excited-state transient Raman spectrum is characterized by the down-shift of the core-size sensitive Raman bands appearing at 1350, 1437, and 1550 cm^{-1} compared with the ground state Raman bands and the prominent enhancement of the pyridine-related bands appearing at 1642, 1249, 1219, 1189, and 792 cm^{-1}. It is well known that the ν_1 and ϕ_4 mode appearing at 1249 and 1642 cm^{-1}, respectively are indicative of the extent of the porphyrin ring-to-aryl charge transfer. The

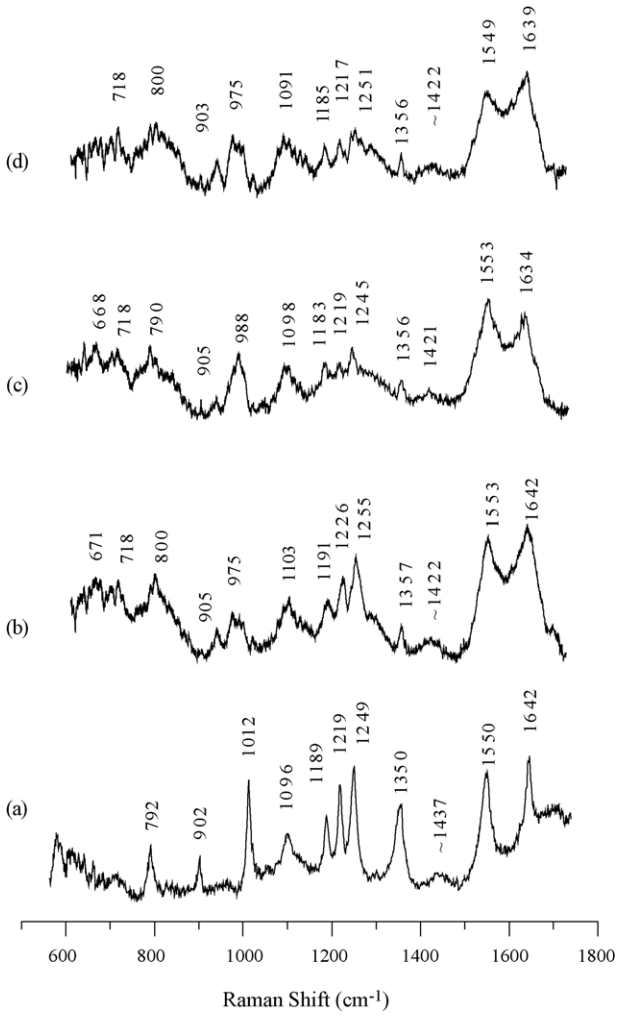

Fig. 5. Nanosecond transient resonance Raman spectra of $OV^{IV}(TMPyP)^{4+}$ with the high power (ca. 0.2 mJ/pulse) both pump and probe pulses at 416 nm: (a) in phosphate buffer solution (pH 7); (b) in poly[d(A-T)$_2$]; (c) in poly[d(G-C)$_2$]; and (d) in calf thymus.

ν_1 mode assigned to C_m-aryl stretching is intense in the triplet state Raman spectrum in parallel with the enhancement of the ϕ_4 mode. The ν_1 mode is expected to be rather insensitive to the geometry of aryl group because the center of mass of the aryl group plays a major role in determining the frequency of this mode. But the ν_1 mode has a contribution from the internal aryl mode that is suggested to arise from the porphyrin ring-to-aryl charge transfer. Thus, the enhancement of the internal aryl mode (ϕ_4 mode) and the ν_1 mode indicates the porphyrins ring-to-aryl charge transfer in the triplet state. Furthermore, the transient Raman bands at 792, 902 and 1012 cm^{-1} are predominantly enhanced in the transient RR spectrum of $OV^{IV}(TMPyP)^{4+}$ in pH 7 aqueous solution. The 792 cm^{-1} band is assigned to the $\nu(CC)_{Pyr}$ and $\nu(N^+–CH_3)$ mode. The 902 cm^{-1} band is assigned to the ν_7 mode, and the band at 1012 cm^{-1} to the ν_6 mode. The C_α–N stretching is mainly responsible for the ν_6 mode, but the C–C stretching in peripheral group contributes considerably to this mode [20]. The ν_7 mode is characterized by the CC deformation in peripheral group. Therefore, the enhancement of these modes also reflects an increased π-electron conjugation between porphyrin plane and peripheral groups probably induced by the rotation of peripheral groups toward porphyrin plane.

On the other hand, in the transient Raman spectrum $OV^{IV}(TMPyP)^{4+}$ in poly[d(G-C)$_2$] (Fig. 5c), the characteristic triplet state bands related to aryl stretching at 1634, 1245, 1219, 1183 and 790 cm^{-1} are very slightly enhanced compared with those in poly[d(A-T)$_2$] and calf thymus (Fig. 5b and d). It has been well established that the enhancement of *meso* substituted phenyl group is characteristic of the triplet state RR spectra of normal- and/or free-base *meso*-tetraphenylporphyrins. The smaller enhancement of Raman bands related to *meso*-aryl of $OV^{IV}(TMPyP)^{4+}$ in poly[d(A-T)$_2$] indicates that the CT state is located at lower energy compared with the triplet state. Therefore, the triplet lifetime of five-coordinated $OV^{IV}(TMPyP)^{4+}$ in poly[d(G-C)$_2$] is shorter than those in other DNA solutions. The lifetime of the triplet state in pH 7 buffer solution was determined to be ca. 66 ns. However, the lifetime of the triplet state in poly[d(G-C)$_2$] as is too fast to be measured by using the laser flash photolysis with ca. 5 ns pulse. The existence of the fast decaying process implies that a certain quenching (Q) state is located lower than the triplet state, and this state acts as deactivation state. The electronic nature of the Q state has not been exactly assigned as to whether it is π–d, d–π or d–d CT states, since there is a lack of experimental evidences on the CT states. However, if the Q state is the π–d CT state, the electronic structure of porphyrin macrocycle in this excited state becomes similar to that of the cationic radical species. In the previously reported Raman spectra of cationic radical of $OV^{IV}TPP$ [15], the ν_2 and ν_4 bands shifted to lower frequencies. Because similar changes were also observed in transient Raman spectra of $OV^{IV}(TMPyP)^{4+}$ in DNA solutions, we suggest that the Q state is the π–d CT state.

The enhancement of *meso*-aryl related Raman bands of $OV^{IV}(H_2O)(TMPyP)^{4+}$ in poly[d(A-T)$_2$] or calf thymus solutions corresponding to the triplet state indicates that the triplet state is located at lower energy rather than the CT state (Fig. 5b and d). Although the transient Raman spectra of its six-coordinated adducts by H_2O ligand can be observed, the difficulty in recording those of its five-coordinated adducts in poly[d(G-C)$_2$] solution gives a clue to address the electronic nature of the main quenching state. The six-coordinated adduct is richer in electron density as compared with the five-coordinated one. Then, the formation of the π–d CT state in the six-coordinated adduct is expected to be less efficient than the five-coordinated one. This explains why the deactivation of six-coordinated adduct is slower than that of the five-coordinated one (Fig. 6).

In conclusion, the polarized spectroscopic studies of $OV^{IV}(TMPyP)^{4+}$ with the polynucleotides demonstrated the groove binding mode of $OV^{IV}(TMPyP)^{4+}$ with DNA and polynucleotides. The Raman features obtained for these complexes are in agreement with the dominant types of the porphyrin interaction with the nucleic acid, i.e., weak external

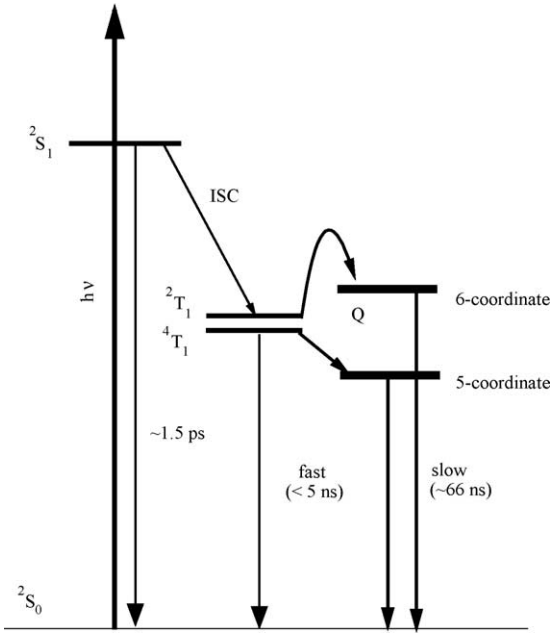

Fig. 6. A proposed energy diagram of $OV^{IV}(TMPyP)^{4+}$ representing the excited-state decay processes and their dynamics. The lifetimes on the excited singlet and triplet state are measured of six-coordinated adduct in pH 7 aqueous solution.

binding in the case of poly[d(A-T)$_2$] and strong external binding in the case of poly[d(G-C)$_2$] expected by the polarized spectroscopy. We conclude that the transient Raman spectroscopy is also useful to probe the differences even in various external binding patterns on the porphyrin-DNA complex. It also releases the detailed information on the photophysical properties of the excited porphyrin-DNA complex.

Acknowledgment

This work was supported by Korean Research Foundation grant (KRF-2002-015-CP0162).

References

[1] R.J. Fiel, J. Biomol. Struct. Dyn. 6 (1989) 1259.
[2] R.F. Pasternack, E. Gibbs, in: T. Tullius (Ed.), Metal DNA Chemistry, Am. Chem. Soc., Washington, DC, 1989.
[3] J.W. Winkleman, in: D. Kessel (Ed.), Advances in Experimental Medicine and Biology, vol. 193, Plenum Press, New York, 1985, pp. 91–96.
[4] J.W. Winkleman, J.H. Collins, Photochem. Photobiol. 46 (1987) 801.
[5] J.E. Critchlow, H.B. Dunford, J. Biol. Chem. 247 (1972) 3714.
[6] J.E. Robert, B.H. Hoffman, R. Rutter, L.P. Hager, J. Am. Chem. Soc. 103 (1981) 7654.
[7] B.W. Griffin, J.A. Peterson, R.W. Estabrook, in: D. Dolphin (Ed.), Porphyrins, vol. 7, Academic Press, New York, 1979, p. 333.
[8] R.E. White, M.J. Coon, Annu. Rev. Biochem. 49 (1980) 315.
[9] R.C. Petterson, L.E. Alexander, J. Am. Chem. Soc. 90 (1968) 3873.
[10] A. Treibs, Angew. Chem. 49 (1936) 682.
[11] R.H. Filby, J.F. Branthaver, Metal complexes in Fossil Fuels, American Chemical Society, Washington, DC, 1987.
[12] D.M. Pai, J. Biol. Chem. 256 (1983) 237.
[13] M. Gouterman, in: D. Dolphin (Ed.), Porphyrins, vol. 3, Academic Press, New York, 1978, p. 78.
[14] M. Gouterman, R.A. Mathies, B.E. Smith, W.S. Caughey, J. Chem. Phys. 52 (1970) 3795.
[15] S.C. Jeoung, D. Kim, S.J. Hahn, S.Y. Ryu, M. Yoon, J. Phys. Chem. 102 (1998) 315.
[16] K. Czarnecki, L.M. Proniewicz, H. Fujii, D. Ji, R.S. Czernuszewicz, J.R. Kincaid, Inorg. Chem. 38 (1999) 1543.
[17] K.A. Macor, R.S. Czernuszewicz, T.G. Spiro, Inorg. Chem. 29 (1990) 1996.
[18] R.G. Alden, L.D. Sparks, M.R. Ondrias, B.A. Crawford, J.A. Shelnutt, J. Chem. Phys. 94 (1990) 1440.
[19] J.A. Shelnutt, M.M. Dobry, J. Phys. Chem. 87 (1983) 3012.
[20] Y.O. Su, R.S. Czernuszewicz, L.A. Miller, T.G. Spiro, J. Am. Chem. Soc. 100 (1988) 4150.
[21] S.C. Jeoung, D. Kim, D.W. Cho, J. Raman Spectrosc. 31 (2000) 319.
[22] S.C. Jeoung, D. Kim, D.W. Cho, M. Yoon, J. Phys. Chem. A 104 (2000) 4816.
[23] B. Nordén, M. Kubista, T. Kurucsev, Q. Rev. Biophys. 25 (1992) 51.
[24] B. Nordén, T. Kurucsev, J. Mol. Recognit. 7 (1994) 141.
[25] A. Rodger, B. Nordén, Circular Dichroism and Linear Dichroism, Oxford University Press, New York, 1997.
[26] (a) Y. Matsuoka, B. Nordén, Biopolymer 21 (1981) 2433;
(b) Y. Matsuoka, B. Nordén, Biopolymer 22 (1982) 1713.
[27] B. Nordén, S. Seth, Appl. Spectrosc. 39 (1985) 647.
[28] M. Lin, M. Lee, K.T. Yue, L.G. Marzilli, Inorg. Chem. 32 (1993) 3217.
[29] J.-O. Kim, Y.-A. Lee, B.H. Yun, S.W. Han, S.T. Kwag, S.K. Kim, Biophys. J. 86 (2004) 1012.
[30] Y.-A. Lee, J.O. Kim, T.-S. Cho, R. Song, S.K. Kim, J. Am. Chem. Soc. 125 (2003) 8106.
[31] N. Blom, J. Odo, K. Nakamoto, D.P. Strommen, J. Phys. Chem. 90 (1986) 2847.
[32] J.-S. Ha, O.-K. Song, M. Yoon, D. Kim, J. Raman Spectrosc. 21 (1990) 667.
[33] O.-K. Song, M. Yoon, D. Kim, J. Raman Spectrosc. 20 (1990) 739.
[34] J.W. Buchler, W. Kokisch, P.D. Smith, Struct. Bonding 34 (1978) 80.
[35] M. Lin, M. Lee, K.T. Yue, L.G. Marzilli, Inorg. Chem. 32 (1993) 3217.